Available online at www.sciencedirect.com
ScienceDirect
Solid State Communications 146 (2008) 181–185
solid state communications
www.elsevier.com/locate/ssc

Electronic structures, lattice dynamics, and electron–phonon coupling of simple cubic Ca under pressure

Guoying Gao[a], Yu Xie[a], Tian Cui[a], Yanming Ma[a,b,*], Lijun Zhang[a], Guangtian Zou[a]

[a] National Lab of Superhard Materials, JiLin University, Changchun 130012, PR China
[b] Laboratory of Crystallography, Department of Materials, ETH Zurich, HCI G 515, Wolfgang-Pauli-Strasse 10, CH-8093 Zurich, Switzerland

Received 6 November 2007; received in revised form 4 January 2008; accepted 21 January 2008 by F. Peeters
Available online 5 February 2008

Abstract

The electronic band structures, lattice dynamics and electron–phonon coupling (EPC) of simple cubic (sc) Ca under pressure have been investigated using first-principles calculations. Analysis of the calculated band structure and Fermi surface with pressure suggests that the predicted electronic topology transitions (ETT) at the X point is mainly responsible for the observed anomaly of the electrical resistance. The phonon calculations for sc Ca with both supercell and linear response methods reveal large imaginary frequencies in the pressure range of 32–109 GPa. This phonon instability might imply the existence of significant anharmonic effect in sc Ca needed to stabilize the crystal. In addition, EPC calculation demonstrates that the observed increase of the superconducting transition temperature T_c with pressure is mainly attributed to the enhancement of the electron density of state at the Fermi level $N(E_F)$ and the EPC matrix element $\langle I^2 \rangle$.

PACS: 71.20.Dg; 71.18.+y; 71.20.-b; 71.38.+i

Keywords: A. Superconductors; D. Electronic band structure; D. Electron–phonon interactions; D. Phonons

1. Introduction

Like other heavy alkaline-earth metals, calcium (Ca) experiences a series of phase transitions under pressure. It adopts a face-centered cubic (fcc) (Ca-I) lattice at ambient conditions. Under compression, it transforms to body-centered cubic (bcc) (Ca-II) and a very unique simple cubic (sc) (Ca-III) structures at 20 GPa and 32 GPa, respectively [1]. The existence of the sc phase in Ca has been theoretically confirmed by total energy calculations [2]. Further experimental measurement [3] suggests that the sc phase exists in a large pressure range of 32–109 GPa. Beyond 110 GPa, two new high-pressure phases of Ca-IV (113–139 GPa) and Ca-V (>139 GPa) have been observed experimentally but not explained theoretically.

The experimental measurements on the electrical resistances of Ca with pressure show two remarkable anomalies [4]. One is the resistance maximum in the 12–19 GPa pressure range [5] within the fcc phase. This abnormal behavior is understandable with the metal–nonmetal transition predicted by the band structure calculations [6,7]. The second anomaly is the obvious discontinuity in resistance at ∼40 GPa within the sc phase [4]. The physical origin for this anomaly remains unknown.

In addition, Ca was found to become a superconductor under pressure similar to Ba [8–11] and Sr [9–12]. The superconductivity of Ca was firstly observed by Dunn [5] as a small drop in the electrical resistance at 2 K and 44 GPa within the sc structure. Later, Shingo et al. [13] demonstrated that the superconducting transition temperature T_c of Ca is below 3 K above 85 GPa and increases linearly with pressure up to 15 K at 150 GPa. A newly published experimental study [4] further showed that T_c reached 25 K at 161 GPa. However, the only theoretical study on the superconductivity of Ca is performed by Shi Lei et al. [14] within the rigid muffin–tin approximation (RMTA). They approximate the mean-square phonon frequency $\langle \omega^2 \rangle$ through the formula $\langle \omega^2 \rangle = 0.5\Theta_D^2$ without considering the distribution of the phonon density of

* Corresponding author at: National Lab of Superhard Materials, JiLin University, Changchun 130012, PR China. Fax: +86 431 85168883.
E-mail address: mym@jlu.edu.cn (Y. Ma).

0038-1098/$ - see front matter © 2008 Elsevier Ltd. All rights reserved.
doi:10.1016/j.ssc.2008.01.026

states (DOS). This approximation leads to much higher T_c than that in experiment.

Normally, the anomaly in the electrical resistance is related to the changes of the electronic properties. This stimulates us to explore the band structures and Fermi surface of sc Ca under compression. In addition, lattice dynamics and electron–phonon coupling (EPC) are calculated to uncover the origin of the pressure-induced T_c enhancement in sc Ca.

2. Computational details

The electronic properties are calculated using the full potential linearized augmented plane wave (LAPW) method through the WIEN2K [15] code. The generalized gradient approximation (GGA) is employed in the electron exchange–correlation energy [16,17]. The muffin–tin radii are chosen to be large enough (2.47 a.u. at ambient conditions) but guarantee that the two muffin–tin spheres do not overlap under pressure. Convergence tests give the choice of kinetic energy cutoff of $Rk_{\max} = 7.0$ and a tetrahedral shifted $17 \times 17 \times 17$ k-point sampling in the Brillouin Zone (BZ). The equation of state (EOS) and lattice dynamics calculations were calculated with pseudopotential plane-wave density-functional theory (DFT) [18,19] through the Quantum-ESPRESSO [20] package. An ultrasoft pseudopotential with the electronic configure of $3s^2 3p^6 4s^2$ was used and the GGA for the exchange–correlation functional [16,17] was employed. Convergence tests gave a kinetic energy cutoff E_{cutoff} as 35 Ry, a $16 \times 16 \times 16$ Monkhorst–Pack (MP) grid for the electronic BZ integration and a dense $24 \times 24 \times 24$ k-mesh is chosen to yield converged phonon frequencies. A $4 \times 4 \times 4$ q mesh in the first BZ was used in the interpolation of theforce constants for the phonon dispersion curve calculations. A supercell method implemented in the PHON [21] program was also employed to further confirm the calculated phonon dispersions. This method uses the Hellmann–Feynman forces calculated from the optimized supercell through the Vienna *ab initio* simulation package (VASP) [22,23] based on DFT within the GGA. Electron ion interaction was represented by the projector augment wave (PAW) method [24], which fully treats all the electrons. Convergence check gave the use of a $4 \times 4 \times 4$ supercell and a $6 \times 6 \times 6$ k mesh in the BZ. The elastic constants are calculated through strain–stress theory by two independent implementations through Cambridge Sequential Total Energy Package (CASTEP) [25] and our own program connected with VASP code. We obtained the elastic constants from evaluations of the stress tensor generated by small strains using the density-functional plane wave technique. In the calculation of elastic constants for both CASTEP and our own implementation, convergence tests give the same kinetic energy cutoffs and k-points sets to be 310.0 eV and a $30 \times 30 \times 30$ uniform Monkhorst–Pack grid, respectively.

The EPC parameter λ was evaluated with the well-known formula [26]

$$\lambda = \frac{N(E_F)\langle I^2 \rangle}{M\langle \omega^2 \rangle}. \tag{1}$$

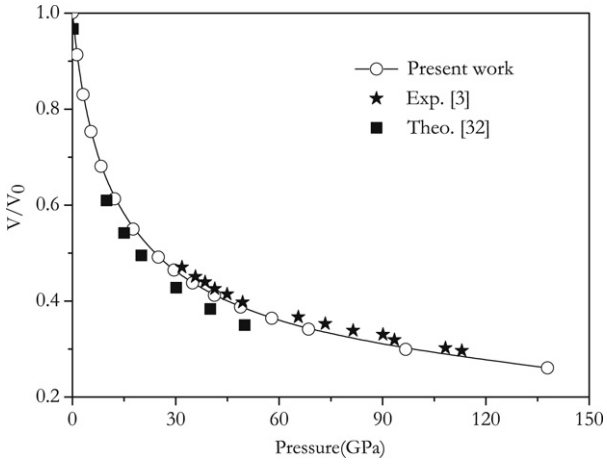

Fig. 1. Calculated EOS is compared with other theoretical results [32] and experimental data [3].

$N(E_F)$ is the electronic DOS per spin at the Fermi level (E_F), $\langle I^2 \rangle$ is the mean square of the electron–ion matrix element averaged over E_F, which is calculated using the RMTA [27,28]. η ($\eta = N(E_F)\langle I^2 \rangle$) is the McMillan–Hopfield [29] parameter, M is the ionic mass and $\langle \omega^2 \rangle$ is an appropriately defined mean-square phonon frequency, which could be derived from the projected phonon DOS [30]. Here the necessary input (muffin–tin sphere potentials, Fermi level, etc.) to the RMTA was generated through the WIEN2K LAPW [15] code.

3. Results and discussions

The EOS of sc Ca shown in Fig. 1 is determined by fitting the total energies as a function of volume to the Murnaghan [31] EOS. Excellent agreement between theory and experiment [3] is found. Note also that the calculated lattice parameter at 39 GPa is 2.634 Å, in a good agreement with the experimental data [1] of 2.615 ± 0.002 Å and the other calculation of 2.649 Å [32]. The good agreement supports the choice of pseudopotential and GGA exchange–correlation functional.

The electronic band structures and two dimensional (2D) Fermi surface under pressure are plotted in Fig. 2. At 32 GPa, it can be clearly seen that there is no energy band crossing over the Fermi level along Γ–X symmetry direction (Fig. 2a), resulting in the absence of Fermi topology along this direction (Fig. 2b). The half-ellipse Fermi surface along X–M (Fig. 2b) is the reflection of the two bands crossing over the Fermi level (Fig. 2a). With increasing pressure, there is no significant change in both band structure (Fig. 2c) and 2D Fermi surface (Fig. 2d) plots, except for the extended half-ellipse towards X due to the pressure-induced lifting of energy band at the X point. At 80 GPa, it is important to note that the degenerate 3d bands at zone center shift below the Fermi level to be occupied and the 4s band lifts over the Fermi level to extend the hole area at the X point as shown in Fig. 2e. Thus, charge transfer from 4s to 3d is seen. Moreover, the dramatic changes in the band structures result in significant modifications of the 2D Fermi surfaces at zone center and the X point (Fig. 2f), respectively, signifying the occurrence of two ETTs. The variations of the